ACS APPLIED MATERIALS & INTERFACES

Research Article

www.acsami.org

Structural Transitions in Asymmetric Poly(styrene)-*block*-Poly(lactide) Thin Films Induced by Solvent Vapor Exposure

Christophe Sinturel,*[,†] David Grosso,[‡] Mickael Boudot,[‡] Heinz Amenitsch,[§] Marc A. Hillmyer,[∥] Alain Pineau,[†] and Marylène Vayer[†]

[†]Centre de Recherche sur la Matière Divisée, CNRS/Université d'Orléans, 1b rue de la Férollerie, 45 071 Orléans Cedex 02, France

[‡]Laboratoire Chimie de la Matière Condensée de Paris, UMR UPMC−CNRS 7574, Université Pierre et Marie Curie (Paris 6), Collège de France, 11 Place Marcelin Berthelot, 75231, Paris, France

[§]Institute of Biophysics and Nanosystems Research, Austrian Academy of Sciences, Schmiedlstr. 6, 8042 Graz, Austria

[∥]Department of Chemistry, University of Minnesota, Minneapolis, Minnesota 55455-0431, United States

Supporting Information

ABSTRACT: Successive structural transitions in thin films of asymmetric poly(styrene)-*block*-poly(lactide) (PS−PLA) block copolymer samples upon exposure to tetrahydrofuran (THF) vapors have been monitored using atomic force microscopy (AFM) and both in situ and ex situ grazing incidence small-angle X-ray scattering (GISAXS). A direct link was established between the structure in the swollen state and the morphology formed in the dried state post solvent evaporation. This was related to the high incompatibility between the constituting blocks of the copolymer that thwarted the system from reaching the homogeneous disordered state in the swollen state under the specific conditions utilized in this study. Upon rapid solvent removal, the morphologies formed in the swollen state were trapped due the fast evaporation kinetics. This work provides a better understanding of the mechanisms associated with block copolymer thin film morphology changes induced by solvent vapor annealing.

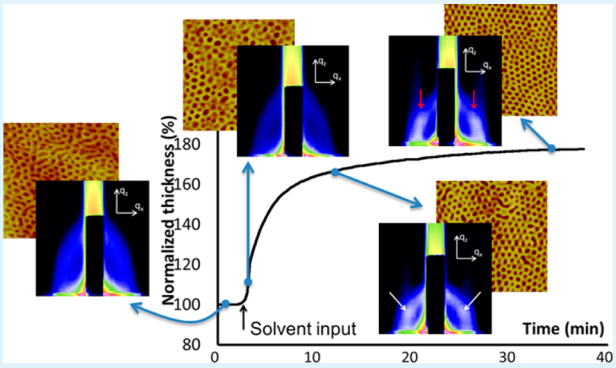

KEYWORDS: *block copolymers, thin films, solvent vapor annealing (SVA), in situ GISAXS, phase transitions*

INTRODUCTION

Ordered thin films of block copolymers have emerged as promising precursors for the fabrication of supported nanostructures with extremely small sizes and precise positional control.[1] In this method, self-assembled block copolymer thin films are used as sacrificial templates to create nanoscale arrays.[2] Among the wide variety of block copolymers that can be used for that purpose, poly(lactide) (PLA) based macromolecules are interesting candidates due to the ease of PLA removal by hydrolytic treatment.[3−7] The Flory−Huggins interaction parameter in PLA-containing block polymers with hydrophobic blocks can be relatively high compared to other systems allowing for smaller domain sizes (at 140 °C $\chi \approx 0.30$ for poly(isoprene)-*block*-poly(lactide), $\chi \approx 0.13$ for poly(styrene)-*block*-poly(lactide), $\chi \approx 0.06$ for poly(styrene)-*block*-poly(methyl methacrylate)).[8] Block copolymer thin films are usually cast from dilute solutions (generally a few weight percent in organic solvent). The resulting films are typically obtained in a nonequilibrium state due to the competition between microphase separation and vitrification as the evaporation of the solvent proceeds.[9,10] Thin films generally adopt disordered structures with little long-range lateral order or orientation of the microdomains.[11] Solvent vapor annealing (SVA) can be applied to improve both the ordering and the orientation of the block copolymer microdomains.[12,13]

In SVA processes, the films are first exposed to organic solvent vapors to form swollen state where the block copolymer mobility is increased, allowing for morphological reorganization. Compared with the thermodynamically stable state obtained in the bulk state, a swollen block copolymer film may adopt a different morphology. This is because the unfavorable segment−segment interactions are modified by the solvent interaction: the structure adopted depends on the extent of swelling, the nature of the solvent and its selectivity for the constituent blocks.[14] Also, in such confined environment (i.e., where the thickness of the film is equal to only a few times the natural period of the block copolymer), the interfacial energy contributions play important roles that can influence the phase diagram of the system.[15] Consequently, depending on the particular solvent/block copolymer interactions and the strength of the interface fields, various morphologies from completely homogeneous disordered to highly oriented order

Received: March 5, 2014
Accepted: July 7, 2014
Published: July 7, 2014

states can be achieved in the film. Only in situ studies can assess the details of the morphologies adopted during swelling and in the swollen state. For that purpose, GISAXS (Grazing Incidence Small Angle X-ray scattering) is one of the most powerful structural characterization techniques.[8,16−19] The conversion of the swollen state to the final dried state occurs after solvent removal.[20] Rapid evaporation of the solvent can "freeze-in" the organization of the swollen state. On the other hand, solvent evaporation can also direct the ordering of the film through the formation of an "ordering front".[21] The structure adopted by a block copolymer film after SVA results from successive phenomena occurring during swelling, in the swollen state and during deswellling. Complete control of the final morphology requires a full understanding of all the structural transitions accompanying these processes.[12,22]

For poly(styrene)-*block*-poly(lactide) (PS−PLA) block copolymers, previous experiments by our group have already shown that well-ordered, perpendicularly oriented cylindrical domains of PLA could be obtained at room temperature through annealing thin PS−PLA films in a tetrahydrofuran (THF) atmosphere.[23] However, the understanding of the process was incomplete since we were not able to conclusively determine the level of swelling and degree of order in the THF swollen films prior to drying. The present work aims to address this issue by performing detailed in situ characterization of the film structure during the solvent annealing process. Although similar experiments have been performed for other systems, there is still the need for new investigations in the area of solvent vapor annealing of block polymers thin films, especially with respect to in situ experimentation. This is because each system can have its own particularities that depend on the block incompatibility, the nature of the solvent and the SVA setup. To control block polymer thin film morphology, there is a great need to understand the behavior in the swollen state and to link it with the dried film.

EXPERIMENTAL SECTION

Materials and Chemicals. Poly(styrene)-*block*-poly(lactide) (PS−PLA) (M_n = 91 kg mol^{-1} by NMR, $Đ$ = 1.07 by SEC vs PS standards) containing a PLA volume fraction of 34% was prepared by a combination of anionic polymerization and ring-opening transesterification polymerization (ROTEP) according to a reported procedure.[3] This block copolymer adopts a hexagonally packed cylindrical morphology at room temperature; with a center to center distance of 58 nm (corresponding to a lattice parameter of 50 nm) and a cylinder diameter of 28 nm.[24]

Substrate Preparation and Spin Coating. The Si substrates (100) were first cleaned by sonication in dichloromethane, methanol, and distilled water for 10 min each, followed by immersion in a HF/HCl/H_2O 1:1:5 solution for 5 min to remove the native oxide layer, then immersed in a $NH_4OH/H_2O_2/H_2O$ 1:1:5 solution. Thin films of PS−PLA were prepared by spin-coating a chlorobenzene solution of PS-*b*-PLA (20 mg mL^{-1}) on Si substrates first at 300 rpm for 15 s and at 2000 rpm for 40 s. Film thicknesses ranged between 110 and 130 nm and were measured by imaging a scratched area in AFM tapping mode or by performing ellipsometric measurements using a UV−visible (240−1000 nm) variable angle spectroscopic ellipsometer (2000U Woollam).

In Situ GISAXS during Solvent Vapor Annealing. The GISAXS measurements were carried out at the Austrian SAXS beamline of Elettra (Trieste-Italy). A monochromatized X-ray radiation source of 8.05 keV (0.154 nm wavelength) was used. The size of the beam was 2 mm in the in plane direction and 200 μm in the off plane direction. The SAXS pattern was collected by a CCD detector (XIDIS, Photonic Science, Grenoble, pixel size 70 μm) placed at 1900 mm from the sample. The calibration of the angular scale was performed with silver behenate $CH_3(CH_2)_{20}$-COOAg (*d*-spacing: 5.838 nm). GISAXS was performed at incident angles above the critical angle of the polymer films (α_c = 0.14° at 0.154 nm). In the sample environment, films were exposed to saturated THF vapors for various times. For that purpose, samples were placed in a closed stainless steel chamber (see Supporting Information) with a total volume of 100 mL at 25 °C with a reservoir of solvent of 25 mL in order to reach in the vessel the saturated vapor pressure of solvent (P_{THF}^0 = 200 mmHg at 25 °C). In the chamber, the sample was placed on a grid, at a distance around 1 cm from the solvent surface. In situ experiments were performed such that one sample was constantly exposed to the THF saturated atmosphere while scattering patterns were collected after 59 s intervals with intervening 1 s acquisition times. This sequence was selected to allow an optimal detection of the microphase structure (optimal signal-to-noise ratio) without deterioration of the molecular structure. A second set of ex situ investigations was performed in which samples were exposed to different periods within the THF vapors before drying and GISAXS analysis. Full width at half-maximum (fwhm) was not used in our case to estimate the degree of long-range order in this configuration due to the anisotropy of the film. Moreover the size of the beam, which a slit in GISAXS, is different after reflection along the in plane and out of plane direction, and depends on the size of the sample and on the incident angle which can vary slightly between samples.[25]

Atomic Force Microscopy (AFM). AFM in the tapping mode was carried out in air at room temperature with a Nanoscope III from Digital Instruments Corp. Silicon cantilevers Tap300 from Budget Sensors with integrated symmetrical pyramidal tips (15 μm high) with no Al coating backside, a nominal spring constant of 42 N·m^{-1} and a resonance frequency between 300−400 kHz were used. All the displayed AFM images are height images taken in tapping mode.

In Situ Ellipsometry upon Solvent Annealing. In situ investigation of the system dynamic of swelling upon THF exposure was achieved using an Environmental Ellipsometer (Woolam VASE 2000U). Block copolymer, or corresponding homopolymer, thin films were introduced into a sealed chamber equipped with nonbirefringent quartz windows, within which the atmosphere was allowed to equilibrate in THF pressure with a small reservoir of liquid THF placed around 1 cm below the polymer thin film sample. The evolutions of the refractive index (n) and of the physical thickness (h) of the films upon THF vapor exposure were then monitored at 25 °C by recording Ψ and Δ between 250 and 1000 nm every 10 s and by fitting the corresponding dispersion with a Cauchy model, well-suited for transparent optical thin dielectric layer. The data allow determination of the rate of THF absorption into the polymer systems. Although the two annealing chambers used for the in situ ellipsometry and the in situ GISAXS were not identical, a careful control of the temperature of the experiment and a placement of the samples at a same distance from the liquid surface make the swelling ratio over time comparable in the two experiments. In the two cases, the atmosphere of the chamber is rapidly saturated by the solvent vapor at a pressure that is then largely dictated by the temperature.

RESULTS AND DISCUSSION

When subjected to SVA conditions, supported polymer thin films swell as a result of solvent adsorption and diffusion of the solvent within the film, leading to a considerable increase of the film thickness. A classical method to monitor such phenomenon is to use environmental ellipsometry,[26,27] as shown in Figure 1 (normalized thickness) for a representative PS−PLA thin film with an initial thickness of 142 nm. As soon as the solvent is injected in the chamber (2 min after starting to record the ellipsometry data), the thickness increases sharply and gradually levels off to reach a plateau after 30 min of exposure. Within the first 10 min, 90% of the total thickness increase was observed. The corresponding variation of polymer volume fraction (dashed line) could be estimated from the thickness variation by assuming a linear dependence with the

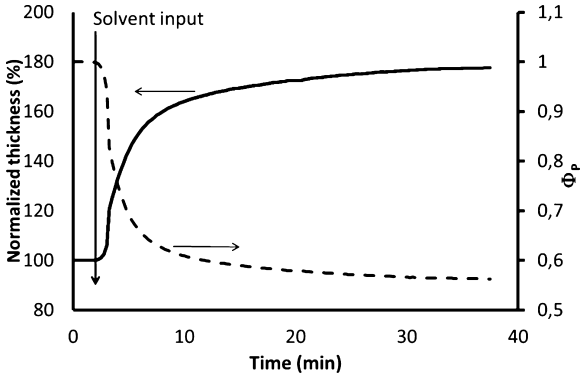

Figure 1. Normalized thickness increase of a PS-*b*-PLA film (absolute initial thickness = 142 nm) upon SVA (solid line, left axis). Polymer volume fraction (Φ_P) in the film (dashed line, right axis).

solvent and copolymer volumes. The polymer fraction decreases down to a value of 0.55 in the plateau.

The data in Figure 1 shows a progressive swelling of the film indicating that the solvent up-take is a limited process. This could represent a solvent front moving through the film, with a gradient of composition in the film. However, the ellipsometry data used to monitor the thickness increase were not fitted with a gradient of composition but with only one homogeneous layer. It indicates that the refractive index is the same through the film profile. Considering that the time needed for the annealing chambers to be equilibrating must rapid (considering their small dimensions) the trend measured in Figure 1 is still unclear.

In order to monitor the morphological changes occurring during the SVA process, scattering patterns were continuously recorded by means of *in situ* GISAXS. The initial film (Figure 2a) exhibits a strong in and off plane radial scattering attributed to randomly oriented PLA domains, characteristic of a poorly ordered system. Upon SVA, the scattering patterns evolve according three major steps that can be illustrated by Figures 2b–e corresponding to 1, 5, 10, and 35 min of SVA (annealing time being taken after the solvent introduction). For short annealing time (Figure 2b and 2c) the scattering patterns contract, mainly in the off plane direction, resulting from thickness increases associated with solvent uptake. For intermediate annealing time (Figure 2d), although the scattered intensity is relatively low given the short acquisition time combined with the naturally low scattering contrast, a change in the diffraction pattern can be observed with the appearance of an out of plane diffraction spot (see white arrows). Longer annealing time leaves only weak vertical diffraction rods (see red arrows in Figure 2e). The absence of high-order Bragg diffraction rods is mainly due to the short acquisition time and weak electron density contrast, particularly in the swollen state. Due to a weak scattering intensity, the form factor was not examined.

This continuous evolution can be seen even clearer in Figure 3 showing the variation of the *in-plane* (q_x) and *out-of plane* (q_z) scattering intensity profiles of GISAXS patterns in the swollen states with time. The line cut in the out of the plane direction q_y was chosen as close as possible of the beamline because most of the intensity of the in-plane diffraction is located behind the beam stop. At this position, we are able to most closely follow the contraction of the network. Both profiles confirm that the solvent swelling occurs most significantly in the off-plane direction. As seen in Figure 3b, a contraction of the diffraction ring along the q_z direction, from 0.23 to 0.11 nm^{-1}, occurs within the first minutes of exposure (<5 min). This corresponds in the real space to a change of the correlation distance from 27 to 57 nm, which can be compared to the value of the lattice parameter in the dry state at equilibrium (50 nm). This indicates that the initial film is far from equilibrium with an out of plane correlation distance considerably smaller. This can be explained by the strong unidirectional contraction occurring upon drying during the spin coating process. As seen in Figure 3a, a much less pronounced increase of the periodicity in the x direction from q_x = 0.12–0.10 nm^{-1} was observed during the same period of annealing (<5 min) and can be attributed to the adhesion of the block copolymer on the

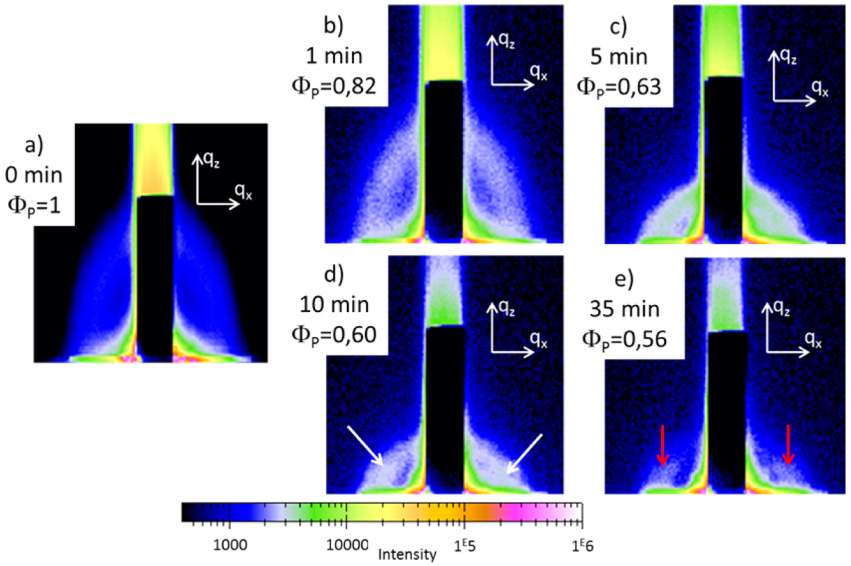

Figure 2. In situ GISAXS patterns on a PS–PLA thin films (initial thickness = 130 nm): initial nonswollen film (a), 1 min (b), 5 min (c), 10 min (d), 35 min (e). The white arrows in c are pointing the (101) diffraction spot of the cubic phase. The red arrows in d are showing diffraction rods generated by the 2D ordered array of PLA cylinders.

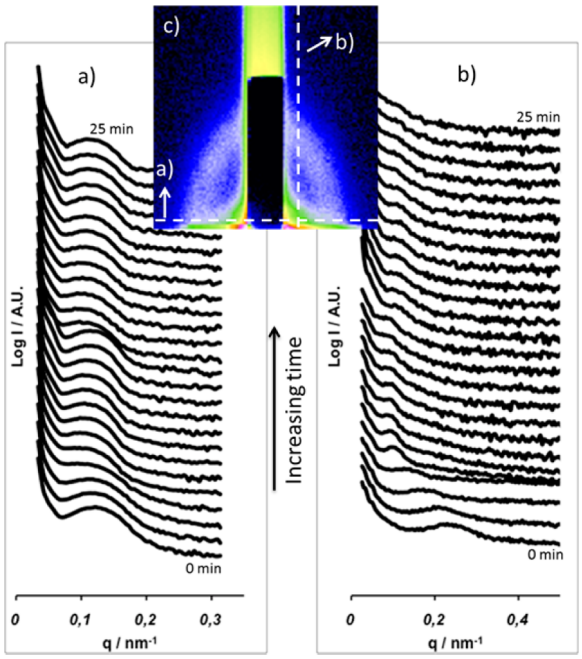

Figure 3. Time dependence of *in-plane* q_x (a) and *out-of plane* q_y (b) GISAXS 1D profile extracted from the in situ characterization (1 min between each plot starting from the bottom). Intensity integrations were made on the white dashed lines on the GISAXS pattern as shown on a typical GI-SAXS pattern obtained after 1 min of THF annealing (c).

surface of the substrate thus limiting lateral expansion upon solvent uptake. When q_z reaches a value that is close to q_x around t = 5 min both q values start to increase but more slowly, suggesting that some structural rearrangement, associated with a reduction of the periodicity degree, may be taking place.

Parts a−e in Figure 4 present images of the surface topography recorded by AFM as well as the corresponding scattering patterns as revealed by the GISAXS, for dry films exposed to various SVA time and quickly removed from the annealing chamber. Under these conditions, the evaporation occurs within few seconds as monitored by ellipsometry. The initial film (Figure 4a) has the typical morphology of a microseparated worm-like state. As shown in the AFM the PLA domains emerge at the surface with circular or elongated shapes, with no evidence of short or long-range order. This apparent disorganized morphology is consistent with a nonequilibrium state, resulting from the fast evaporation of the solvent during spin-casting. After increasing time of SVA, the dried films morphology progressively evolves as probed by AFM and GISAXS. For short solvent exposure times (1 and 5 min) the reorganization is insignificant and a poorly ordered state is still observed. Improved level of organization is observed by AFM after 10 and 35 min of exposure. Corresponding GISAXS data exhibit a very different internal reorganization of the film with scattering patterns exhibiting a clear out of plane diffraction spot (white arrows) for 10 min and sharp in-plane Bragg peaks (red arrows) for 35 min. The change in degree of order after 10 min as compared to 35 min of SVA is interesting since over that time frame there is very little change in the content of solvent in the film (Figure 1). This can due to the time for the polymer to equilibrate but it can also be noted that small changes in degree of swelling can impact polymer chain conformation.

From our previous study,[23] it is known that the degree of organization in PS−PLA spin coated thin films is a function of the SVA time, evolving from a disordered state to perpendicular

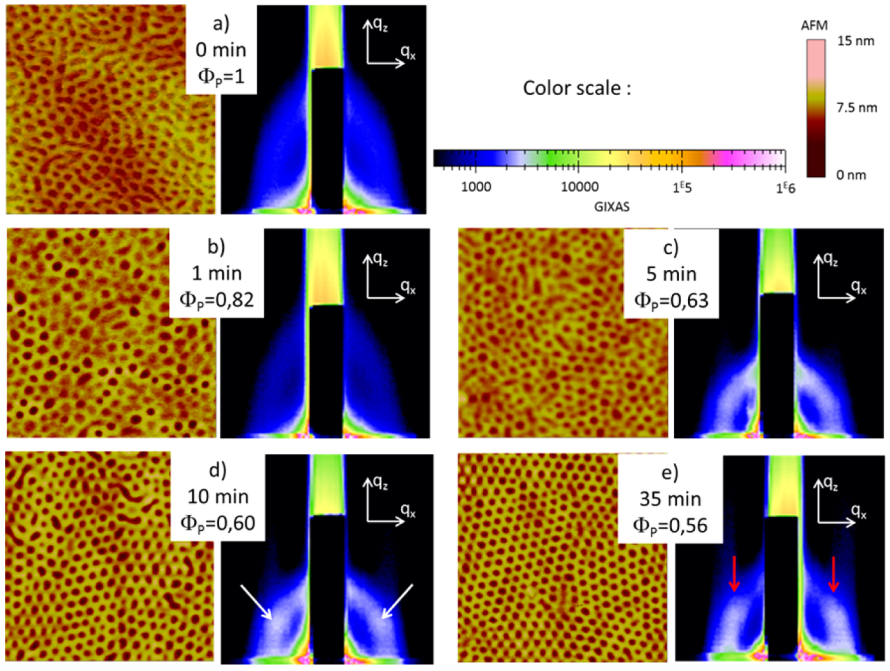

Figure 4. Ex situ AFM and GISAXS of films annealed for 0, 1, 5, 10, and 35 min (respectively a, b, c, d, and e) and quickly removed from the annealing chamber. Φ_P is the polymer volume fraction in the swollen state. All AFM images are 1 μm × 1 μm, with the same vertical scale bar. All GISAXS patterns are presented with the same q_x (in plane, horizontal) and q_z (out of plane, vertical) range ($-0.3 < q_x < 0.3$; $0 < q_z < 0.5$) in log scale intensity with same color scale for all images. The white arrows in part d point to the (101) diffraction spot of the cubic phase. The red arrows in e show diffraction rods generated by the 2D ordered array of PLA cylinders.

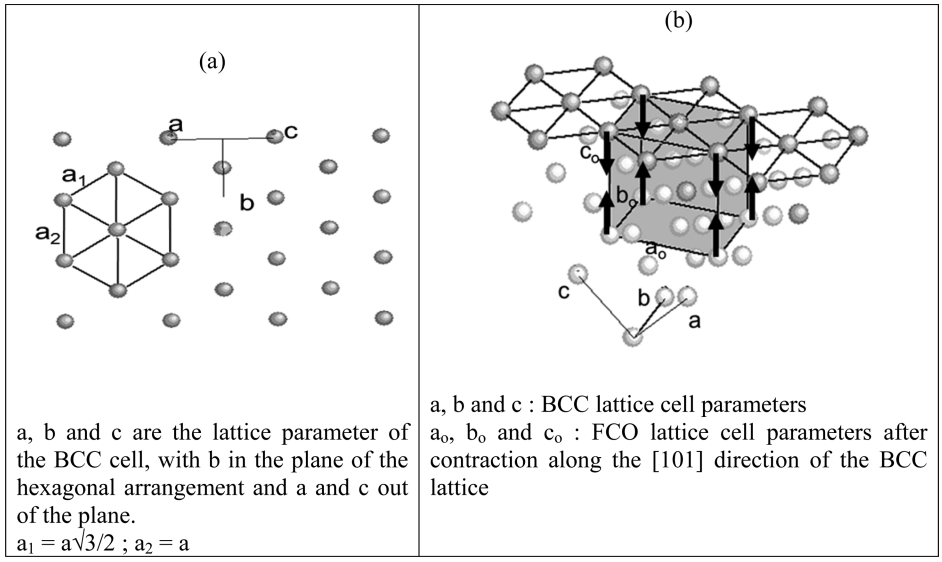

Figure 5. View of the sphere lattice after the solvent evaporation. Plan view (a), three-dimensional view (b).

array of ordered cylinders. Such behavior is herein confirmed, but it is also suggested that the system undergoes more complex behavior with intermediates structural transitions. The in situ GISAXS patterns recorded upon SVA, together with the morphological characterization of the dried states is now discussed in order to propose a pathway for the structural reorganization of the studied PS−PLA thin films upon SVA.

A first observation that can be drawn from the in situ scattering patterns is that the swollen state remains microphase-separated. Despite a drop of the intensity due to a dilution effect upon swelling, a significant amount of scattered signal is preserved upon SVA indicating that the homogeneous disordered state of the phase diagram is not reached under these particular conditions where the polymer volume fraction does not go below 0.56. This is consistent with recent work on PS−PLA solutions in THF[28] but it differs from other block polymers/solvent pairs where self-organization is lost (e.g., PS-*b*-PEO in benzene vapors[21]). This is certainly related to the relatively high value of the Flory−Huggins parameter $\chi_{PS/PLA}$ (0.22 at 25 °C) and the relatively high molar mass of the PS−PLA used. It is also worth noting that, for a given time of exposure, the GISAXS patterns in the swollen state and in the dried state are very similar, suggesting that the rapid evaporation step freezes the swollen state morphology. Although the evaporation step may influence the dried morphology,[29] the relatively high molar mass of the polymer used in this study could significantly slow morphological rearrangement within the time scale of the evaporation.

In addition to the expected GISAXS patterns of the disordered wormlike and ordered hexagonally packed array of cylinders respectively observed at short and long SVA time, we have observed a singular scattering pattern with a clear out of plane diffraction spot (see white arrows in Figures 2d and 4d). The simulations of the GISAXS patterns of the same block copolymer have been performed by our group.[30] For this system, we have clearly identified the disordered, the perpendicular as well as the parallel cylindrical morphologies by comparing the experimental and the simulated data. It is clear that the scattering obtained in this study, for intermediate scattering time, with distinct out of plane diffraction spots, is different from the morphologies depicted in our previous work. Consistent with other inorganic[31] or polymer[32,33] systems, we have assigned this diffraction pattern to the typical out of plane (101) diffraction spot of a body centered cubic phase (bcc) cubic phase with the [110] direction of the domains normal to the surface. We also propose that the change in the periodicity at t = 5 min (Φ_P = 0.63 in the present experiment) is due to the transition from a wormlike state to a bcc state that is retained during the rapid solvent evaporation. Such phenomenon is consistent with transformation of the hexagonally packed cylindrical phase toward the bcc phase upon swelling that has been shown in other systems such as poly(*α*-methylstyrene)-*block*-poly(4-hydroxystyrene)[32] and poly(styrene)-*block*-poly(4-vinylpiridine).[33] In our case, such phenomenon could be explained by a preferential swelling of the PS phase that would decrease the PLA/PS volume ratio, which could in turn cause a morphological shift. However, the solvent/polymer interaction parameter for THF is indeed relatively similar for the both blocks (0.4 and 0.6 for χPS/THF and χPLA/THF, respectively), thus we consider THF a relatively neutral solvent. Moreover, we have observed with pure thin films of PS and PLA, that PLA swells more with THF than the PS under the same conditions (see Supporting Information). Consequently, the phase transition reported here is more likely attributed to a mediation of the blocks incompatibility due to a dilution effect of the nonselective solvent, leading to a reduction of the effective interaction parameter, allowing for more facile structural transitions. It should be noted that grains with parallel-oriented cylinders buried in the films could also contribute to the diffraction spots in the first and second quadrants.[8] Such buried morphology could be missed by the AFM observations that only provide the extreme surface morphology. Although this hypothesis cannot be fully discard since we do not have direct evidence of the internal morphology, our previous works on the subjects have demonstrated that parallel orientations were formed at much higher SVA time.[23]

Upon fast drying, a 3D lattice of spheres is maintained in the film, as revealed by the GISAXS pattern of the dried state (Figure 4e). This is apparently not supported by the corresponding AFM image (Figure 4e) that exhibits a morphology that could be easily attributed to hexagonally

packed perpendicular cylinders. However, since AFM can probe only the top layer of the films, the observed circular features can be interpreted as spheres or cylinders perpendicular to the surface. It is then not possible to distinguish between those two different types of domains with AFM alone. Moreover, if we consider that the surface of the dried film is formed from the [101] plane of the bcc lattice of the swollen state, the spheres will appear at the surface in a "distorted" hexagonal lattice, which will be difficult to distinguish from a true hexagonal lattice (see Figure 5a). Also, it should be noted that in our conditions (thickness of the film above the natural period of the polymer), we assume that we are not in the conditions of a monolayer of spheres that would favor the hexagonal Wigner–Seitz (W–S) cell of sphere.[34,35] Under deswelling, unlike other systems where the spherical morphology collapses to perpendicular cylindrical morphology,[33] the system in our experimental conditions is trapped in a 3D spherical morphology obtained via a unidirectional contraction of a bcc lattice. This is consistent with the fact that the direction of contraction occurs along the [101] direction and not along the [111] direction (the closest-packed direction in a bcc lattice), which normally become the cylinder long axis in a typical transition from spheres to cylinders with an epitaxial relationship, as shown previously.[36−38] This mismatch, associated with rapid solvent evaporation, freezes the morphology. Finally, it can be seen from the GISAXS pattern, that the sphere lattice parameters in the dry state are different from those monitored in the swollen state. This can be explained by the film evaporation-induced-shrinkage that will mainly affect the spacing of the spheres in the direction perpendicular to the surface, leading to a distorted bcc lattice or more accurately to a face-centered orthorhombic (FCO) lattice of spheres (Figure 5b).[31]

For longer annealing times, the GISAXS patterns (Figures 2e and 4e) indicate that the spherical lattice is no longer stable: hexagonally packed perpendicular cylinders are formed in the swollen state indicating that the spherical lattice was only a transitional phase. This is consistent with the fact that the film still swells after the formation of the bcc phase (Figure 1). Although the volume change is minor between 10 and 35 min, further shifts in morphology are possible. As already mentioned, small changes in degree of swelling can impact polymer chain conformations. After the mediation of the interaction between the blocks that accounts for the drop of the effective interaction parameter leading to a first structural transition hex to bcc, the change of the relative volume fraction of the swollen domains may be sufficient to allow for the system to re-enter the hex phase. This was confirmed by studying the swelling of the homopolymers that shows different swelling behavior (see Supporting Information).

CONCLUSION

In this work, we forward a new understanding in the mechanisms of the morphology changes produced by THF annealing of PS–PLA thin films. For this block copolymer, we demonstrated that the variety of morphologies obtained during SVA was mainly driven by the phenomenon occurring in the swollen state. A clear link was established between the structure in the swollen state and the morphology formed in the dried state, after solvent evaporation. This was related to the high incompatibility and relatively high molar mass between the constituting block of the polymer, not allowing the system to reach, in the swollen state, the homogeneous disordered state of the phase diagram under the conditions explored. In the swollen state, we also pointed out an original reversible phase transition from hexagonally packed cylinders to sphere of PLA arranged in bcc lattice. The bcc was found to be only an intermediate state, obtained for intermediate swelling extent. Very interestingly, we showed that this bcc arrangement could be transferred to the dried matrix, with a surface pattern (as seen by AFM) very close to the hex phase. This study confirms that in situ studies are crucial in the domains of SVA in order to bring a complete understanding of the process. For that purpose, GISAXS, used in combination with more conventional observation technique (such as SEM or AFM), is particularly well adapted.

ASSOCIATED CONTENT

Supporting Information

3D illustration of the GISAXS annealing chamber (Figure S1). Normalized thickness increase of PLA and PS homopolymer thin films (Figure S2). This material is available free of charge via the Internet at http://pubs.acs.org/.

AUTHOR INFORMATION

Corresponding Author

*Email: christophe.sinturel@univ-orleans.fr.

Notes

The authors declare no competing financial interest.

ACKNOWLEDGMENTS

We thank the reviewers for their helpful comments on the original version of this paper. The University of Orléans, the CNRS, and the Ministry of Higher Education and Research are acknowledged for supporting polymer research at the CRMD. M.A.H. acknowledges LE STUDIUM for his research fellowship in residence at Université d'Orléans/CNRS, on sabbatical leave from the University of Minnesota. Christian Morello at the synchrotron Elettra is thanked for the conception of the in situ annealing chamber used in the GISAXS line.

REFERENCES

(1) Park, C.; Yoon, J.; Thomas, E. L. Enabling Nanotechnology with Self Assembled Block Copolymer Patterns. *Polymer* **2003**, *44*, 6725–6760.

(2) Kao, J.; Thorkelsson, K.; Bai, P.; Rancatore, B. J.; Xu, T. Toward Functional Nanocomposites: Taking the Best of Nanoparticles, Polymers, and Small Molecules. *Chem. Soc. Rev.* **2013**, *42*, 2654–2678.

(3) Zalusky, A. S.; Olayo–Valles, R.; Taylor, C. J.; Hillmyer, M. A. Mesoporous Polystyrene Monoliths. *J. Am. Chem. Soc.* **2001**, *123*, 1519–1520.

(4) Zalusky, A. S.; Olayo–Valles, R.; Wolf, J. H.; Hillmyer, M. A. Ordered Nanoporous Polymers from Polystyrene–Polylactide Block Copolymers. *J. Am. Chem. Soc.* **2002**, *124*, 12761–12773.

(5) Bucholz, T. L.; Li, S. P.; Loo, Y.-L. Ultra-Low-κ Materials Derived from Poly(D,L-Lactide-*b*-Pentafluorostyrene) Diblock Copolymers. *J. Mater. Chem.* **2008**, *18*, 530–536.

(6) Majdoub, R.; Antoun, T.; Le Droumaguet, B.; Benzina, M.; Grande, D. Original Route to Polylactide–Polystyrene Diblock Copolymers Containing a Sulfonyl Group at the Junction Between Both Blocks as Precursors to Functional Nanoporous Materials. *React. Funct. Polym.* **2012**, *72*, 495–502.

(7) Dirany, M.; Vayer, M.; Sinturel, C.; Erre, R.; Lacroix-Desmazes, P.; Boutevin, B. Synthesis and Characterization of Polystyrene-*block*-Polylactide by Combination of ATRP and ROP Using Tribromoethanol as Initiator: Precursors to Ordered Nanoporous Materials. *J. Appl. Polym. Sci.* **2011**, *122*, 2944–2951.

(8) Cavicchi, K. A.; Russell, T. P. Solvent Annealed Thin Films of Asymmetric Polyisoprene−Polylactide Diblock Copolymers. *Macromolecules* **2007**, *40*, 1181−1186.
(9) O'Driscoll, S.; Demirel, G.; Farrell, R. A.; Fitzgerald, T. G.; O'Mahony, C.; Holmes, J. D.; Morris, M. A. The Morphology and Structure of PS-*b*-P4VP Block Copolymer Films by Solvent Annealing: Effect of the Solvent Parameter. *Polym. Adv. Technol.* **2011**, *22*, 915−923.
(10) Hamley, I. W. Ordering in Thin Films of Block Copolymers: Fundamentals to Potential Applications. *Prog. Polym. Sci.* **2009**, *34*, 1161−1210.
(11) Tang, C.; Tracz, A.; Kruk, M.; Zhang, R.; Smilgies, D.-M.; Matyjaszewski, K.; Kowalewski, T. Long-Range Ordered Thin Films of Block Copolymers Prepared by Zone-Casting and Their Thermal Conversion into Ordered Nanostructured Carbon. *J. Am. Chem. Soc.* **2005**, *127*, 6918−6919.
(12) Sinturel, C.; Vayer, M.; Morris, M.; Hillmyer, M. Solvent Vapor Annealing of Block Polymer Thin Films. *Macromolecules* **2013**, *14*, 5399−5415.
(13) Ming Luo, M.; Epps, T. H. Directed Block Copolymer Thin Film Self-Assembly: Emerging Trends in Nanopattern Fabrication. *Macromolecules* **2013**, *46*, 7567−7579.
(14) Nandan, B.; Vyas, M. K.; Böhme, M.; Stamm, M. Composition-Dependent Morphological Transitions and Pathways in Switching of Fine Structure in Thin Films of Block Copolymer Supramolecular Assemblies. *Macromolecules* **2010**, *43*, 2463−2473.
(15) Knoll, K.; Lyakhova, K. S.; Horvat, A.; Krausch, G.; Sevink, G. J. A.; Zvelindovsky, A. V.; Magerle, R. Direct Imaging and Mesoscale Modelling of Phase Transitions in a Nanostructured Fluid. *Nat. Mater.* **2004**, *3*, 886−890.
(16) Cavicchi, K. A.; Berthiaume, K. J.; Russell, T. P. Solvent Annealing Thin Films of Poly(isoprene-*b*-lactide). *Polymer* **2005**, *46*, 11635−11639.
(17) Paik, M. Y.; Bosworht, J. K.; Smilges, D. M.; Schwartz, E. L.; Xavier, A.; Ober, C. K. Reversible Morphology Control in Block Copolymer Films via Solvent Vapor Processing: An in Situ GISAXS Study. *Macromolecules* **2010**, *43*, 4253−4260.
(18) Di, Z.; Posselt, D.; Smilgies, D.-M; Li, R.; Rauscher, M.; Potemkin, I. I.; Papadakis, C. M. Stepwise Swelling of a Thin Film of Lamellae-Forming Poly(styrene-*b*-butadiene) in Cyclohexane Vapor. *Macromolecules* **2012**, *45*, 5185−5195.
(19) Gu, X.; Gunkel, I.; Hexemer, A.; Gu, W.; Russell, T. P. An In Situ Grazing Incidence X-Ray Scattering Study of Block Copolymer Thin Films During Solvent Vapor Annealing. *Adv. Mater.* **2014**, *26*, 273−281.
(20) Albert, J. N. L.; Young, W.-S.; Lewis, R. L.; Bogart, T. D.; Smith, J. R.; Epps, T. H. Systematic Study on the Effect of Solvent Removal Rate on the Morphology of Solvent Vapor Annealed ABA Triblock Copolymer Thin Films. *ACS Nano* **2012**, *6*, 459−466.
(21) Kim, S. H.; Misner, M.; Xu, T.; Kimura, M.; Russell, T. P. Highly Oriented and Ordered Arrays from Block Copolymers via Solvent Evaporation. *Adv. Mater.* **2004**, *16*, 226−231.
(22) Phillip, W. A.; Hillmyer, M. A.; Cussler, E. L. Cylinder Orientation Mechanism in Block Copolymer Thin Films Upon Solvent Evaporation. *Macromolecules* **2010**, *43*, 7763−7770.
(23) Vayer, M.; Hillmyer, M. A.; Dirany, M.; Thevenin, G.; Erre, R.; Sinturel, C. Perpendicular Orientation of Cylindrical Domains Upon Solvent Annealing Thin Films of Poly(styrene)-*b*-Poly(lactide). *Thin Solid Films* **2010**, *518*, 3710−3715.
(24) Vayer, M.; Nguyen, T.-H.; Grosso, D.; Boissiere, C.; Hillmyer, M. A.; Sinturel, C. Characterization of Nanoporous Polystyrene Thin Films by Environmental Ellipsometric Porosimetry. *Macromolecules* **2011**, *44*, 8892−8897.
(25) Faustini, M.; Nicole, L.; Boissière, C.; Innocenzi, P.; Sanchez, C.; Grosso, D. Hydrophobic, Antireflective, Self-Cleaning, and Antifogging Sol-Gel Coatings: An Example of Multifunctional Nanostructured Materials for Photovoltaic Cells. *Chem. Mater.* **2010**, *22*, 4406−4413.
(26) Zettl, U.; Knoll, A.; Tsarkova, L. Effect of Confinement on the Mesoscale and Macroscopic Swelling of Thin Block Copolymer Films. *Langmuir* **2010**, *26*, 6610−6617.
(27) Knoll, A.; Margele, R.; Krausch, G. Phase Behavior in Thin Films of Cylinder-Forming ABA Block Copolymers: Experiments. *J. Chem. Phys.* **2004**, *120*, 1105−1116.
(28) Kim, J. C.; Seo, M.; Hillmyer, M. A.; Francis, L. F. Magnetic Microrheology of Block Copolymer Solutions. *ACS Appl. Mater. Interfaces* **2013**, *5*, 11877−11883.
(29) Paradiso, S. P.; Delaney, K. T.; García-Cervera, C. J.; Ceniceros, H. D.; Fredrickson, G. H. Block Copolymer Self Assembly during Rapid Solvent Evaporation: Insights into Cylinder Growth and Stability. *ACS Macro Lett.* **2014**, *3*, 16−20.
(30) Nguyen, T. H.; Vayer, M.; Grosso, D.; Amenitsch, H.; Sinturel, C. Using Sol-Gel Replications to Assess the Porosity of Block-Copolymer Derived Thin Films. *J. Phys. Chem. C* **2012**, *116*, 5295−5302.
(31) Grosso, D.; Soler-Illia, G. J. De A. A.; Crepaldi, E. L.; Cagnol, F.; Sinturel, C.; Bourgeois, A.; Brunet-Bruneau, A.; Amenitsch, H.; Albouy, P.; Sanchez, C. Highly Porous TiO_2 Anatase Optical Thin Films with Cubic Mesostructure Stabilized at 700 °C. *Chem. Mater.* **2003**, *15*, 4562−4570.
(32) Bosworth, J. K.; Paik, M. Y.; Ruiz, R.; Schwartz, E. L.; Huang, J. Q.; Ko, A. W.; Smilgies, D.-M.; Black, C. T.; Ober, C. K. Control of Self-Assembly of Lithographically Patternable Block Copolymer Films. *ACS Nano* **2008**, *2*, 1396−1402.
(33) Gowd, E. B.; Böhme, M.; Stamm, M. In Situ GISAXS Study on Solvent Vapor Induced Orientation Switching in PS-*b*-P4VP Block Copolymer Thin Films. *Synchrotron Radiation in Polymer Science* **2010**, *14*, 012015.
(34) Matsen, M. W. The Standard Gaussian Model for Block Copolymer Melts. *J. Phys. Condens. Mater.* **2002**, *14*, R21−R47.
(35) Yao, L.; Woll, A. R.; Watkins, J. J. Directed Assembly of Block Copolymer Templates for the Fabrication of Mesoporous Silica Films with Controlled Architectures via 3-D Replication. *Macromolecules* **2013**, *46*, 6132−6144.
(36) Sota, N.; Hashimoto, T. Process and Kinetics of Order−Order Transition from bcc-Sphere to hex-Cylinder in Polystyrene-*block*-Polyisoprene-*block*-Polystyrene: Time-Resolved SAXS and TEM Studies. *Polymer* **2005**, *46*, 10392−10404.
(37) Ryu, C. Y.; Lodge, T. P. Thermodynamic Stability and Anisotropic Fluctuations in the Cylinder-to-Sphere Transition of a Block Copolymer. *Macromolecules* **1999**, *32*, 7190−7201.
(38) Mykhaylyk, T. A.; Mykhaylyk, O. O.; Collins, S.; Hamley, I. W. Ordered Structures and Phase Transitions in Mixtures of a Polystyrene/Polyisoprene Block Copolymer with the Corresponding Homopolymers in Thin Films and in Bulk. *Macromolecules* **2004**, *37*, 3369−3377.